ROBUST DIGITAL SELF-INTERFERENCE CANCELLATION FOR FULL-DUPLEX UWA SYSTEMS: LAKE EXPERIMENTS

Lu Shen, Benjamin Henson, Yuriy Zakharov, Paul Mitchell

Department of Electronic Engineering, University of York, YO10 5DD, UK

Lu Shen, Department of Electronic Engineering, University of York, YO10 5DD, UK
Email: ls1215@york.ac.uk

Abstract: *Full-duplex (FD) underwater acoustic (UWA) communication has significant potential in increasing the capacity of acoustic links, but it suffers from severe self-interference (SI) caused by the near-end transmission. Existing SI cancellation techniques include analogue cancellation, digital cancellation and antenna beamforming. Among those techniques, the digital cancellation has the lowest complexity. However, the reported digital SI cancellation performance is limited. To improve performance, the non-linearity of the power amplifier (PA) should be taken into account. Here we use the digitized PA output as the reference signal for SI estimation to reduce the effect of the non-linear distortion. Such a system architecture allows us to use a low-complexity linear adaptive filter for SI cancellation. Specifically, we use the recursive least-squares (RLS) algorithm with dichotomous coordinate descent (DCD) iterations. This results in a low-complexity SI canceller. As observed from the experimental results with traditional single-branch digital canceller, the choice of the sampling time is crucial to the SI cancellation performance. In this paper, we present a robust digital SI cancellation scheme based on the RLS-DCD algorithm with the use of the PA output. To achieve robust SI cancellation performance, the PA output is oversampled to twice the symbol rate, de-multiplexed into two branches employing digital SI cancellation, and then combined based on the residual variance estimates in the two branches. The SI cancellation performance is investigated by conducting experiments in an indoor water tank and in a shallow lake. The tank experiments show that up to 66 dB of SI can be cancelled using the proposed scheme, which is high compared to existing FD designs. Meanwhile, up to 56 dB of SI is cancelled in the lake experiments. The difference in the SI cancellation performance is due to faster varying SI channels in the lake experiments. Both the water tank and lake experimental results show robust SI cancellation performance regardless of the choice of sampling time.*

Keywords: *Digital cancellation, full-duplex, field experiments, self-interference cancellation, underwater acoustic communication*

1. INTRODUCTION

Acoustic waves are the best candidate for long-range underwater communications [1]. However, the attenuation of acoustic waves is approximately proportional to the square of the frequency, which makes the available bandwidth for underwater acoustic (UWA) communications extremely limited [2] [3]. Furthermore, the usable frequency range of acoustic transducers and limited bandwidth (<1 kHz) for long-range communication (>1 km) impose additional constraints on the available frequency resources [2] [4]. To increase the capacity of acoustic links, we consider full-duplex (FD) UWA communications, when the transceiver simultaneously transmits and receives in the same frequency bandwidth. With FD operation, it is possible to increase the channel capacity [5] [6]. The major obstacle of FD communication is the strong self-interference (SI) introduced by the near-end transmission [7] [8] . For long-distance UWA communication with high transmission power, the SI can be millions of times stronger than the far-end desired signal.

Existing SI cancellation techniques for FD terrestrial radio communications include analogue cancellation, digital cancellation and antenna beamforming [8] [9] [10]. For terrestrial radio designs, a combination of analogue and digital cancellation is normally used to avoid saturation of the analogue-to-digital converter (ADC). For FD UWA systems, the low signal frequency allows the use of high resolution ADCs (e.g., 24 bits). In such a case, we intend to achieve a high level of SI cancellation in the digital domain. The major factor which affects the performance of digital cancellation is the non-linear distortion introduced by the power amplifier (PA). Existing designs [9] [10] deal with the PA non-linearity by using the Volterra series [11] and its extensions to model the nonlinear SI channel, which are of high complexity. We adopt a low-complexity digital canceller design by using the PA output as the reference signal [12]. In this case, a linear digital canceller can be sufficient, since the non-linear distortion introduced by the PA is incorporated in the reference signal. Specifically, the digital canceller is implemented using a low-complexity recursive least-squares (RLS) adaptive filter with dichotomous coordinate descent (DCD) iterations [13] [14].

From our investigation, another important issue which affects the performance of the digital canceller is the choice of the sampling time. When the sampling time is not properly chosen, the SI cancellation performance degrades significantly (see Fig. 2). To ensure robust cancellation performance, the PA output is sampled at two shifted sampling times. In that case, we obtain two time-shifted copies of the baseband PA output and these are used as the reference signal to perform digital cancellation on two branches independently. The two residual signals are then combined with weight coefficients, computed based on the residual variance estimates. The general idea of the combining scheme is to ensure that the combined residual signal is at the same level as in the branch with better cancellation performance.

The SI cancellation performance is investigated by conducting experiments in an indoor water tank and in a shallow lake. The tank experiments show that up to 66 dB of SI could be cancelled with the proposed digital canceller. Meanwhile, up to 56 dB of SI is cancelled in the lake experiments. The difference in the cancellation performance can be attributed to faster time-variation of the SI channel in the lake, which could be further improved by combining digital cancellation with other approaches, such as adaptive beamforming.

2. SYSTEM MODEL

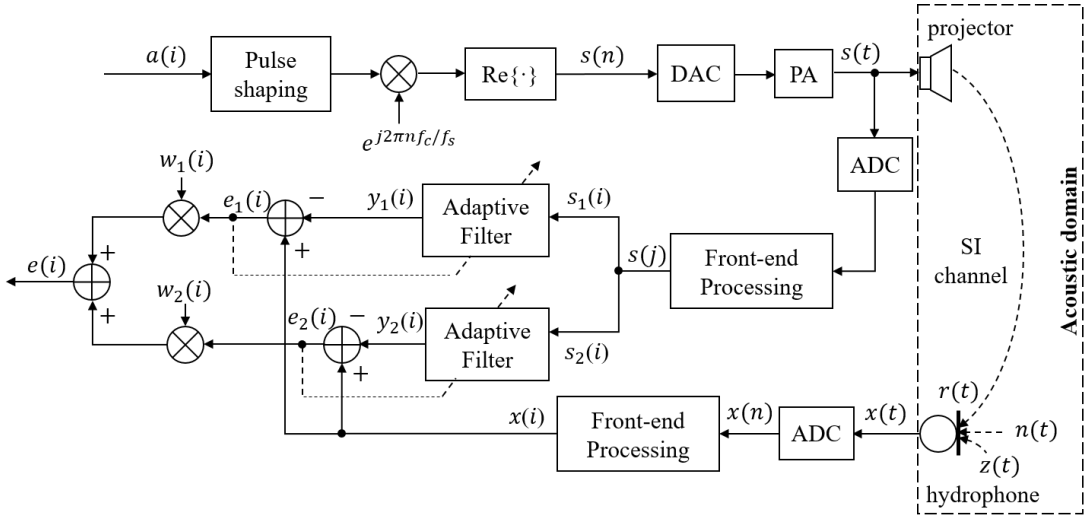

Fig.1: Block diagram of the FD UWA system. The sample index with sampling rate f_s, symbol rate f_d and $2f_d$ are denoted by n, i and j, respectively.

The block diagram of the FD UWA system with digital cancellation is shown in Fig. 1. We transmit a pseudo-random sequence of BPSK data symbols $a(i)$. The symbol rate is f_d. The BPSK data is up-sampled to a high sampling frequency f_s by a pulse-shaping filter, modulated to the carrier frequency f_c. The passband signal $s(n)$ is digital-to-analogue converted, amplified in a PA and emitted by an acoustic projector. The received signal $x(t)$ at the near-end hydrophone includes the SI signal $r(t)$, ambient noise $n(t)$ and far-end signal $z(t)$.

For SI channel estimation, we use the RLS-DCD adaptive filter, which is chosen for its low-complexity, fast convergence and numerical stability (see details in [13] [14]). The residual signal is computed by subtracting the adaptive filter output from the received signal. The adaptive filter works at the symbol rate to reduce the computational complexity and to avoid the ill-condition problem of the narrowband regressor [15].

We use the baseband equivalent received signal $x(i)$ as the desired signal for both adaptive filters. To obtain the baseband equivalent signal, the digitalized received signal $x(n)$ is demodulated to the baseband, low-pass filtered and decimated to f_d (in the front-end processing block). A pair of root-raised cosine (RRC) filters are used for pulse shaping and low-pass filtering.

From our observation, the sampling time is crucial for the SI cancellation performance. In Fig. 2, we show the mean-squared error (MSE) performance of a single branch with different choice of sampling time. We consider 4×96 different sampling time instants within 4 symbol intervals (4 ms), where each symbol contains 96 samples. It can be seen that the MSE performance is sensitive to the sampling time within one symbol duration. As high as 40 dB difference in the MSE performance can be observed. Similar phenomenon is also reported in [16] regarding the equalizer performance in a band-limited channel. To ensure robust MSE performance, the digitalized PA output $s(j)$ is oversampled to twice the symbol rate ($2f_d$). The digital samples of $s(j)$ are de-multiplexed into two branches. The signal $s_1(i)$ in the first branch contain odd samples, while $s_2(i)$ in the second branch contain even samples. $s_1(i)$ and $s_2(i)$ are used as the regressors of the two adaptive filters in the first and second branch, respectively. Note that the sampling delay shift between two branches is half a symbol duration. In that case, we can ensure that good cancellation performance can be achieved with at least one of the branches according to Fig. 2.

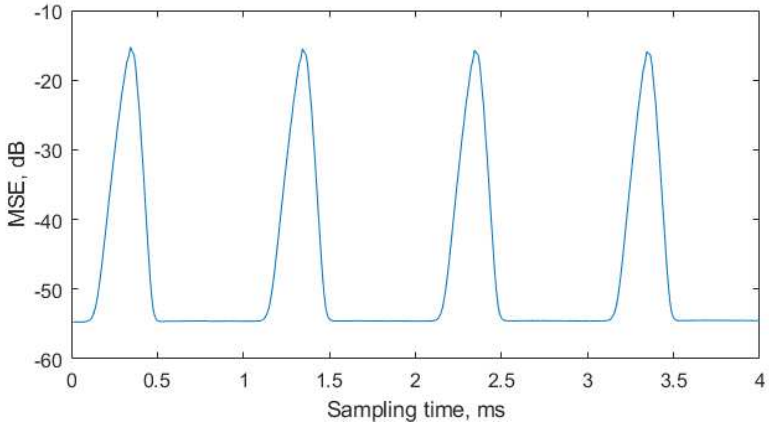

Fig.2: MSE performance with different sampling time using lake experimental data.

After digital cancellation, the residual signals $e_1(i)$ and $e_2(i)$ are combined with different weight coefficients which are computed based on the residual variance estimates in the two branches. The variance on the kth branch ($k = 1, 2$) at the ith time instant is estimated by:

$$\sigma_k^2(i) = \alpha\sigma_k^2(i-1) + (1-\alpha)|e_k(i)|^2, \tag{1}$$

where α is a forgetting factor. The weight coefficients $w_k(i)$ are then computed by:

$$w_k(i) = \frac{1}{\sigma_k^2(i)} \Big/ \left(\frac{1}{\sigma_1^2(i)} + \frac{1}{\sigma_2^2(i)}\right), \qquad k = 1, 2. \tag{2}$$

According to the combining scheme, a small weight coefficient is applied to the branch with high variance (residual signal power), and a large weight coefficient is applied to the branch with high level of SI cancellation. As the sum of the weights equals to one, the level of the received signal is not changed after combining. With this approach, robust SI cancellation performance can be achieved at any sampling time.

3. EXPERIMENTAL RESULTS

In this section, we investigate the SI cancellation performance in the water tank and lake experiments. The tank experiments are conducted in a 38cm×119cm×42cm indoor water tank. During the experiments, the projector [17] and hydrophone [18] are clamped by a retort stand, separated by 4cm and submerged underwater as shown in Fig. 3.

Fig.3: Configuration of the water tank experiments.

We transmit BPSK data with a sampling frequency of $f_s = 96$ kHz and a carrier frequency of $f_c = 12$ kHz. The frequency bandwidth is $F_d = 1$ kHz. The RRC filter we use has a roll-off factor of 0.2 and a filter length of 14 symbols duration (14 ms). A Hanning window is applied to the RRC filter taps to achieve higher attenuation at the passband. The transmitted signal length is 15 s, which includes 5 s of zero padding at the beginning of the signal. This silence period is used to measure the background noise level. Here we use the steady-state normalized MSE (NMSE) level as the indicator for the cancellation performance. The NMSE level at the kth branch ($k = 1, 2$) is computed by:

$$\text{NMSE}(i) = \frac{P_e}{P_x} = \frac{|e_k(i)|^2}{P_x}, \tag{3}$$

where $P_x = \sum_{i=0}^{N-1} |x(i)|^2 / N$ is the average power of the desired signal of the adaptive filter, N is the length of the desired signal, P_e is the instantaneous power of the residual signal $e_k(i)$. The NMSE level after combining is computed by:

$$\text{NMSE}(i) = \frac{P_{e_c}}{P_x} = \frac{|e(i)|^2}{P_x}, \tag{3}$$

where P_{e_c} is the instantaneous power of the combined residual signal $e(i)$. The steady-state NMSE is computed by averaging the NMSE over the last five seconds of the signal.

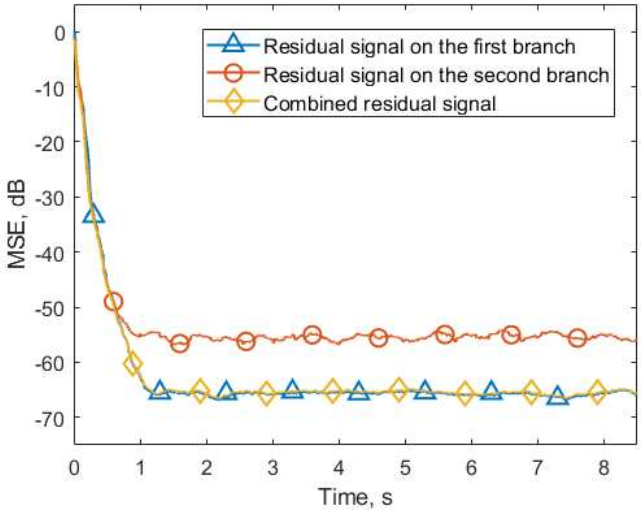

Fig. 4: Averaged NMSE performance in the tank experiment.

Fig. 4 shows the NMSE performance in the tank experiment. The NMSE curve is smoothed by averaging the instantaneous NMSE over a period of 0.3 s to provide a clearer view. The length of the adaptive filter is $L = 100$ (about 100 ms), which is long enough to capture the SI channel delay spread. The forgetting factor is $\lambda = 0.995$. The parameters of the DCD iterations are chosen as follows: the number of bits representing the impulse response $M_b = 16$, and the number of DCD updates $N_u = 4$. The forgetting factor used for the variance estimation is $\alpha = 0.95$. For the first branch, the steady-state NMSE is around -66 dB, while in the second branch the NMSE level is about 10 dB higher than in the first branch. As can be seen in Fig. 4, the NMSE level of the combined residual signal is approximately the same as that in the first branch after combining the signals in the two branches, showing the effectiveness of the combining scheme.

To evaluate the SI cancellation performance in a more practical scenario, lake experiments were conducted. The experimental site is shown in Fig. 5. In the lake experiments, the projector and the hydrophone are placed at a depth of 0.5 m, the distance between them is 3 cm (see Fig. 6).

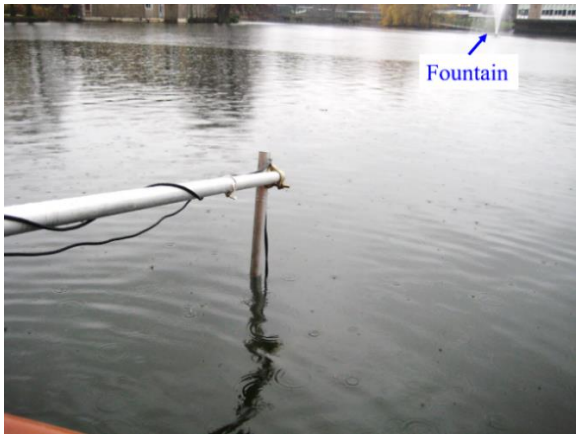

Fig. 5: Experimental site for the lake experiments.

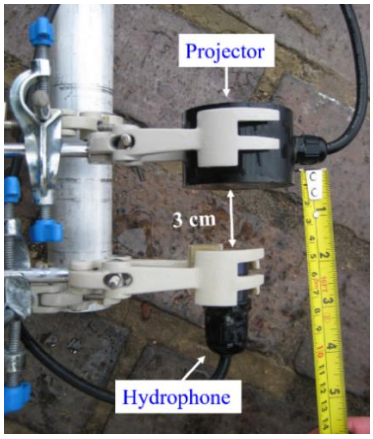

Fig. 6: Experimental setup

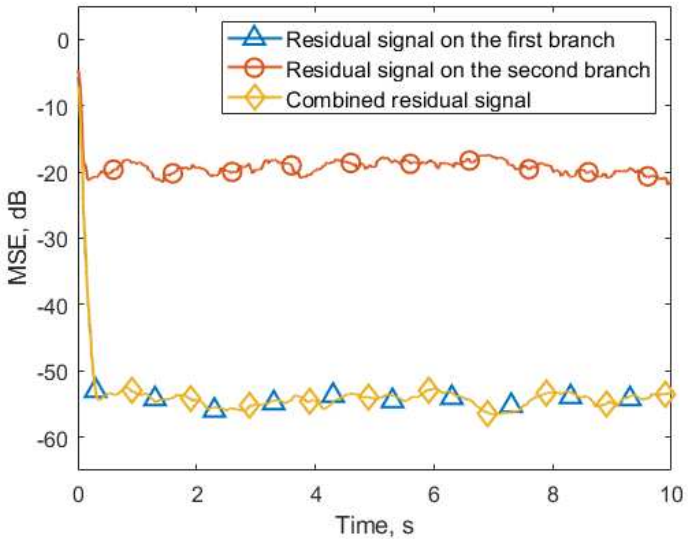

Fig. 7: Averaged NMSE performance in the lake experiment.

The NMSE performance in the lake experiment is shown in Fig. 7. The NMSE curve is smoothed by averaging the instantaneous NMSE over a period of 0.5 s. The averaging time window used here is longer compared to that of the tank experiment (0.3 s). This is due to the larger fluctuations in the MSE curve, which are caused by faster time-variation of the SI channel in the lake. We use an adaptive filter length of $L = 60$, and a forgetting factor $\lambda = 0.985$. As less number of reflections are received in the lake, a shorter filter length is used. For the DCD iterations, the number of bits representing the impulse response $M_b = 16$, and the number of DCD updates $N_u = 4$. The forgetting factor used for the residual variance estimate is $\alpha = 0.9$. It can be seen that the steady-state NMSE in the first branch is around -54 dB. For the second branch, the NMSE performance is significantly worse. After combining, the NMSE level of the combined residual signal is at the same level as that of the first (better) branch.

Note that for both the tank and lake experiments, the RLS-DCD algorithm achieves the same steady-state NMSE level as the classical RLS algorithm, but with significantly lower

complexity. The experimental results in the water tank and lake experiments demonstrate that robust and high level SI cancellation can be achieved with the proposed digital cancellation scheme regardless of the sampling time. The lower level of SI cancellation achieved in the lake experiments can be explained by faster SI channel variation in the lake experiments attributed by several environmental factors, including the time-varying lake surface. Another factor which limits the cancellation performance in the experiments could be the potential non-linear distortion introduced by the projector and the hydrophone, which is not being cancelled by the linear digital canceller [19].

4. CONCLUSION

In this paper, we investigate the SI cancellation performance of the proposed digital cancellation scheme in both water tank and lake experiments. The digital canceller is implemented using the low-complexity RLS-DCD adaptive filter with the PA output used as the reference signal for the SI channel estimation. The PA output is oversampled by two and de-multiplexed into two branches. The digital canceller is applied in each branch. The residual signals after digital cancellation are combined with different weights based on the residual variance estimate on two branches. This de-multiplexing and combining scheme is used to deal with the sensitivity of the SI cancellation performance to the sampling time. As demonstrated by the experimental results, effective and robust SI cancellation is achieved with the proposed digital cancellation scheme.

5. ACKNOWLEDGEMENTS

The work of B. Henson, Y. Zakharov and P. Mitchell was supported in part by the U.K. EPSRC through Grants EP/P017975/1 and EP/R003297/1.

REFERENCES

[1] **M. Stojanovic**, "Underwater acoustic communications," in *IEEE Electro International. Professional Program Proceeding*, 1995.

[2] **I. F. Akyildiz, D. Pompili and T. Melodia**, "Underwater acoustic sensor networks: Research challenges," *Ad Hoc Networks,* vol. 3, pp. 257-279, 2005.

[3] **T. H. Eggen, A. B. Baggeroer and J. C. Preisig**, "Communication over Doppler spread channels. Part I: Channel and receiver presentation," *IEEE Journal of Oceanic Engineering,* vol. 25, pp. 62-71, 2000.

[4] **M. Stojanovic and J. Preisig**, "Underwater acoustic communication channels: Propagation models and statistical characterization," *IEEE communications magazine,* vol. 47, pp. 84-89, 2009.

[5] **G. Qiao, S. Gan, S. Liu, L. Ma and Z. Sun**, "Digital Self-Interference Cancellation for Asynchronous In-Band Full-Duplex Underwater Acoustic Communication," *Sensors,* vol. 18, pp. 1700-1716, 2018.

[6] **G. Qiao, S. Liu, Z. Sun and F. Zhou**, "Full-duplex, multi-user and parameter reconfigurable underwater acoustic communication modem," in *MTS/IEEE Oceans*, 2013.

[7] **D. W. Bliss, P. A. Parker and A. R. Margetts**, "Simultaneous transmission and reception for improved wireless network performance," in *IEEE Workshop on Statistical Signal Processing*, 2007.

[8] **J. I. Choi, M. Jain, K. Srinivasan, P. Levis and S. Katti**, "Achieving single channel, Full duplex wireless communication," in *International Conference on Mobile Computing and Networking*, 2010.

[9] **D. Bharadia, E. McMilin and S. Katti**, "Full duplex radios," in *ACM SIGCOMM Computer Communication Review*, 2013.

[10] **D. Korpi, Y. S. Choi, T. Huusari, L. Anttila, S. Talwar and M. Valkama**, "Adaptive nonlinear digital self-interference cancellation for mobile inband full-duplex radio: Algorithms and RF measurements," in *IEEE Global Communications Conference*, 2015.

[11] **A. Zhu and T. J. Brazil**, "Behavioral modeling of RF power amplifiers based on pruned Volterra series," *IEEE Microwave and Wireless Components Letters,* vol. 14, pp. 563--565, 2004.

[12] **L. Shen, B. Henson, Y. Zakharov and P. Mitchell**, "Digital self-interference cancellation for underwater acoustic systems," *IEEE Transactions on Circuits and Systems II: Express Briefs,* 2019, In Press.

[13] **Y. V. Zakharov, G. P. White and J. Liu**, "Low-complexity RLS algorithms using dichotomous coordinate descent iterations," *IEEE Transactions on Signal Processing,* vol. 56, pp. 3150-3161, 2008.

[14] **J. Liu, Y. V. Zakharov and B. Weaver**, "Architecture and FPGA design of dichotomous coordinate descent algorithms," *IEEE Transactions on Circuits and Systems I: Regular Papers,* vol. 56, pp. 2425-2438, 2009.

[15] **S. S. Haykin**, Adaptive Filter Theory, Prentice Hall, 2002.

[16] **J. G. Proakis and M. Salehi**, Digital Communications, McGraw-Hill, 2008.

[17] "Low frequency underwater transducer," [Online]. Available: https://www.benthowave.com/products/BII-7530lowfrequencytransducer.html. [Accessed 29 March 2019].

[18] "Low Noise Broadband Hydrophone," [Online]. Available: https://www.benthowave.com/products/BII-7010Hydrophone.html. [Accessed 29 March 2019].

[19] **J. Butler and C. Sherman**, Transducers and Arrays for Underwater Sound, Springer International Publishing, 2016.